

# ULRR


## Role of thermal and photoannealing on nonlinear optical response of Ge<sub>30</sub>Se<sub>55</sub>Bi<sub>15</sub> thin films

Item Type	Article
Authors	Aparimita, Adyasha;Khan, Pritam;Aswin, J.R.;Adarsh, K.V.;Naik, R.
Citation	Journal of Applied Physics;127, 075102
Publisher	American Institute of Physics
Download date	2026-04-16 15:24:14
Item License	<a href="https://creativecommons.org/licenses/by-nc-sa/1.0/">https://creativecommons.org/licenses/by-nc-sa/1.0/</a>
Link to Item	<a href="https://hdl.handle.net/10344/8656">https://hdl.handle.net/10344/8656</a>

# Role of thermal and photoannealing on nonlinear optical response of $\text{Ge}_{30}\text{Se}_{55}\text{Bi}_{15}$ thin films

Cite as: J. Appl. Phys. **127**, 075102 (2020); <https://doi.org/10.1063/1.5132579>

Submitted: 18 October 2019 . Accepted: 03 February 2020 . Published Online: 18 February 2020

Adyasha Aparimita, P. Khan, J. R. Aswin, K. V. Adarsh, and R. Naik 



View Online



Export Citation



CrossMark

## ARTICLES YOU MAY BE INTERESTED IN

[Influence of oxygen-rich and zinc-rich conditions on donor and acceptor states and conductivity mechanism of ZnO films grown by ALD—Experimental studies](#)

Journal of Applied Physics **127**, 075104 (2020); <https://doi.org/10.1063/1.5120355>

[Structural properties and magnetoresistance of  \$\text{La}\_{1.952}\text{Sr}\_{0.048}\text{CuO}\_4\$  thin films](#)

Journal of Applied Physics **127**, 073901 (2020); <https://doi.org/10.1063/1.5139719>

[Thermal hysteresis and its impact on the efficiency of first-order caloric materials](#)

Journal of Applied Physics **127**, 075103 (2020); <https://doi.org/10.1063/1.5132897>

Lock-in Amplifiers  
Find out more today



 Zurich Instruments



# Role of thermal and photoannealing on nonlinear optical response of Ge<sub>30</sub>Se<sub>55</sub>Bi<sub>15</sub> thin films

Cite as: J. Appl. Phys. 127, 075102 (2020); doi: 10.1063/1.5132579

Submitted: 18 October 2019 · Accepted: 3 February 2020 ·

Published Online: 18 February 2020



Adyasha Aparimita,<sup>1</sup> P. Khan,<sup>2</sup> J. R. Aswin,<sup>3</sup> K. V. Adarsh,<sup>3</sup> and R. Naik<sup>1,4,a)</sup> 

## AFFILIATIONS

<sup>1</sup>Department of Physics, Utkal University, Vanivihar, Bhubaneswar 751004, India

<sup>2</sup>Department of Physics and Bernal Institute, University of Limerick, V94 T9PX Limerick, Ireland

<sup>3</sup>Department of Physics, Indian Institute of Science Education and Research, Bhopal 462023, India

<sup>4</sup>Department of Engineering and Material Physics, ICT-IOC Odisha campus, Bhubaneswar 751013, India

<sup>a)</sup>Author to whom correspondence should be addressed: ramakanta.naik@gmail.com

## ABSTRACT

In this article, we employed the nanosecond Z-scan technique to demonstrate the nonlinear optical response in Ge<sub>30</sub>Se<sub>55</sub>Bi<sub>15</sub> thin films after thermal and photoannealing. The intensity dependent open aperture Z-scan traces reveal that all the samples, i.e., as-prepared, thermal, and photoannealed thin films, exhibit reverse saturable absorption. The experimental results indicate that both thermal and photoannealing can be efficiently used to enhance the nonlinear absorption coefficient ( $\beta$ ) compared to the as-prepared sample. We further demonstrate that the  $\beta$  value of thermally annealed and as-prepared samples increases significantly at higher intensities. On the contrary, the  $\beta$  value of the photoannealed sample does not exhibit appreciable changes against the intensity variation.

Published under license by AIP Publishing. <https://doi.org/10.1063/1.5132579>

## I. INTRODUCTION

Amorphous chalcogenide glasses (ChGs) stand apart from their counterpart optical materials because of their unique linear and non-linear optical properties. For example, they possess high linear refractive indices<sup>1</sup> (2.0–3.0 at 1.55  $\mu\text{m}$ ) and high third order nonlinear refractive index ( $\sim 1000$  times that of silica).<sup>2,3</sup> The latter has attracted significant interest in theoretical and experimental investigations owing to their numerous applications in various fields, which includes optical limiting,<sup>4</sup> optical switching,<sup>5</sup> multi-photon polymerization,<sup>6</sup> photo-dissolution,<sup>7</sup> etc. To date, most of the previous experiments exploring the non-linear optical properties have been conducted on Ge and As-based ChGs.<sup>8–10</sup> For example, Huang *et al.* observed strong enhancement in third order non-linearities as a result of the formation of defect-like bonds in Ge–Sn–Se chalcogenide glasses.<sup>11</sup> On the other hand, Smektala *et al.* demonstrated a strong variation of the nonlinear refractive index in As<sub>2</sub>S<sub>3</sub> and As<sub>2</sub>Se<sub>3</sub> glasses with the input laser intensity.<sup>12</sup>

In spite of high photosensitivity of ChGs, their application gets limited because of poor thermal stability. An efficient way to overcome such an issue is doping third impurity elements such as Bi, Sb with more metallic character into the ChG matrix, which can improve the thermal stability significantly with added functionalities.<sup>13,14</sup>

For example, with the incorporation of metallic Bi, the glass formation region gets expanded and stabilized for the Ge–Se–Bi system.<sup>15</sup> The chemical durability and IR transmission also increase by the addition of Bi into the Ge–Se system. Nevertheless, for practical applications, it is important to tune the linear and non-linear optical properties of the Ge–Se–Bi system. Thermal and photoannealing are considered to be efficient techniques to alter the linear and non-linear optical constants of ChGs. Although the effect of such annealing has been studied on the linear optical properties, the implications remain unknown for the non-linear optical response.

To gain new insights into the third order non-linear optical properties of Ge–Se–Bi ChGs upon thermal and photoannealing, we employed the conventional open aperture Z-scan technique. Z-scan traces reveal that upon resonant excitation of 1064 nm, all the samples, i.e., as-prepared, thermal, and photoannealed samples, undergo reverse saturable absorption (RSA). A comparative study reveals that non-linear absorption coefficient ( $\beta$ ) increases significantly upon thermal and photoannealing.

## II. EXPERIMENTAL

The bulk Ge<sub>30</sub>Se<sub>55</sub>Bi<sub>15</sub> was prepared by using the melt quench technique from the high pure elements Ge, Se, and Bi (5N, Aldrich

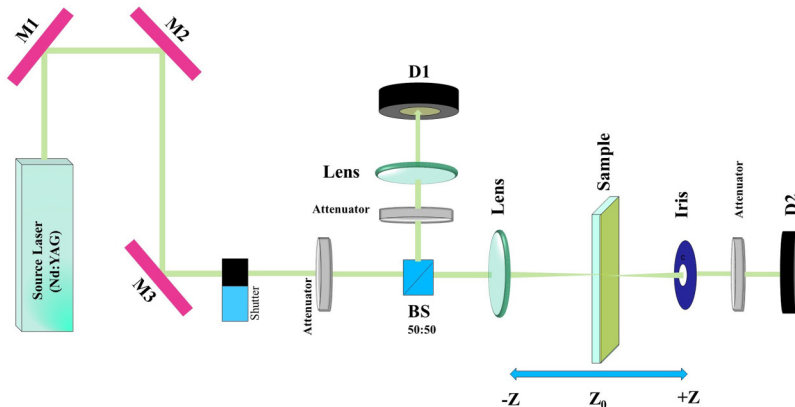


FIG. 1. Schematic diagram of the open aperture Z-scan technique.

and Sigma Chemical Company). The highly pure elements were weighted in the stoichiometric ratio and placed into a pre-cleaned quartz ampoule. The ampoule was then sealed under vacuum at a pressure of about  $\sim 5 \times 10^{-4}$  Torr. The ampoules were placed in a programmable rocking furnace and slowly heated up to  $950^\circ\text{C}$  for about 36 h with continuous gentle rocking to ensure homogeneity. After full homogenization of the melt, the ampoules were rapidly quenched in ice cold water.

Thin films of  $\text{Ge}_{30}\text{Se}_{55}\text{Bi}_{15}$  were deposited from the prepared bulk material by the thermal evaporation technique on glass substrates at a base pressure of  $\sim 5 \times 10^{-5}$  Torr. The substrate temperature was maintained at room temperature, and the deposition rate was fixed at 5 nm per second during the deposition process. The substrates were rotated slowly to get a homogeneous and uniform film. We prepared films of thickness  $\sim 1\ \mu\text{m}$ , confirmed from thickness crystal monitor. The films were thermally annealed for 2 h at  $120^\circ\text{C}$ . For photoannealing, the sample was irradiated with a 532 nm continuous wave laser for  $\sim 2$  h with an illumination intensity of  $50\ \text{mW cm}^{-2}$ .

To explore the nonlinear optical properties of the films, we employed the open aperture Z-scan technique, which measures the total transmittance as a function of incident laser intensity. The schematic diagram of the open aperture Z-scan technique is presented in Fig. 1. In this method, the thin films were illuminated

with 1064 nm, 5 ns pulses of Nd:YAG laser. We used a fixed repetition rate of 10 Hz to avoid sample heating and photo-damage.

### III. RESULTS AND DISCUSSIONS

First, we investigated the effect of thermal and photoannealing on the linear optical properties of as-prepared  $\text{Ge}_{30}\text{Se}_{55}\text{Bi}_{15}$  thin films by recording the optical absorption spectra of the samples as shown in Fig. 2(a). The optical absorption coefficient ( $\alpha$ ) was calculated from the absorbance spectra from the following formula:<sup>16</sup>

$$\alpha = \frac{2.303A}{t}, \quad (1)$$

where  $A$  and  $t$  are the absorbance and the thickness of the thin film, respectively. Then, we calculated the optical bandgap of each sample by using the Tauc equation<sup>17</sup>

$$(ah\nu) = B(h\nu - E_g)^2, \quad (2)$$

where  $\alpha$ ,  $h$ ,  $\nu$ ,  $E_g$ , and  $B$  are the absorption coefficient, Planck's constant, frequency, optical bandgap, and a constant (Tauc parameter), respectively. A straight-line fitting of the plot  $(ah\nu)^{1/2}$

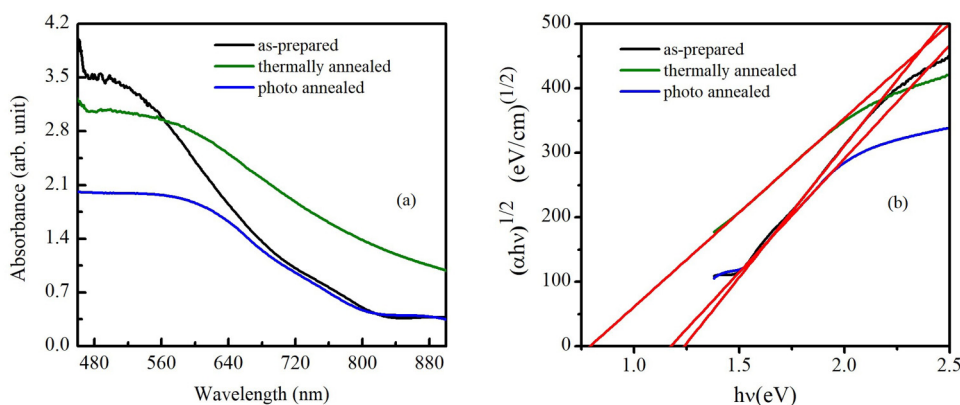


FIG. 2. (a) Optical absorbance spectra of the as-prepared, thermally, and optically annealed films. (b) The Tauc plot for the respective films for the calculation of the bandgap.

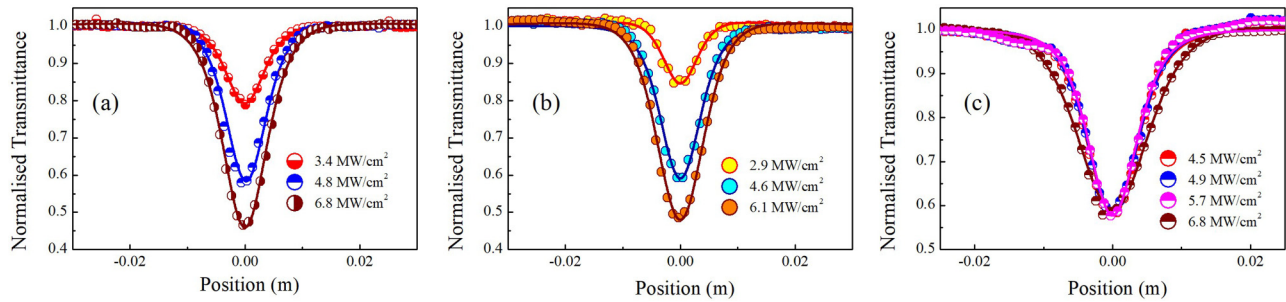


FIG. 3. Normalized transmittance as a function of input intensity of (a) as-prepared (b) thermally annealed (c) photoannealed  $\text{Ge}_{30}\text{Se}_{55}\text{Bi}_{15}$  thin films.

vs  $h\nu$  to the energy axis gives the value of optical bandgap, which is shown for all samples in Fig. 2(b).

From the Tauc plot, the bandgaps are found to be 1.22, 0.77, and 1.17 eV for as-prepared, thermally annealed, and photoannealed  $\text{Ge}_{30}\text{Se}_{55}\text{Bi}_{15}$  films, respectively. Clearly, the optical bandgap decreases upon thermal and photoannealing. The decrease in the bandgap upon thermal annealing can be explained by the Mott and Davis model, which says that the width of the localized states and bandgap depend on the degree of disorderness and defects present in the amorphous structure.<sup>18</sup> When the as-prepared sample is thermally annealed below the glass transition temperature, additional dangling bonds are formed, which leads to the formation of the defect states. Consequently, the width of localized states increases, which eventually results in a decrease in bandgap for the thermally annealed films. On the other hand, the reduction in optical bandgap by photoannealing is the direct consequence of the conventional photodarkening process<sup>19,20</sup> and the effect of which is less than the thermal annealing. We believe that the tunability of the optical bandgap<sup>21</sup> of the sample can be useful for many optical devices.

In spite of the promising linear optical properties of ChGs as active materials in optoelectronic devices, an extremely important issue to be addressed is non-linear optical properties, which makes them a favorable candidate to fabricate several non-linear optical devices. In this regard, we present an interpretation of the

third-order nonlinear  $[\chi(3)]$  optical properties of as-prepared, thermally, and optically annealed  $\text{Ge}_{30}\text{Se}_{55}\text{Bi}_{15}$  chalcogenide thin films.

We employed the conventional open aperture Z-scan technique to unveil the non-linear optical properties. In this context, Figs. 3(a)–3(c) show the open aperture Z-scan traces at three peak intensities of resonant excitation at 1064 nm for as-prepared, thermally and photoannealed  $\text{Ge}_{30}\text{Se}_{55}\text{Bi}_{15}$  thin films, respectively. At these very low intensities, for all the samples, the normalized transmittance shows a gradual decrease when the position of the sample (Z) approaches zero (focal point). The least possible value of transmittance at the focal point is represented by the dip in the normalized transmittance curve. Such curves clearly illustrate that RSA takes place in our sample similar to the observation of Elim *et al.*<sup>22</sup> RSA has many potential applications in optical pulse compressor, optical switching, laser pulse narrowing, etc.<sup>22</sup> With the increase in laser intensity, the transmittance decreases gradually, which is a typical behavior of optical limiting process that plays an important role in protecting optoelectronic detectors as well as the human eye from intense laser sources.<sup>23</sup>

To quantify the RSA process, we computed the non-linear absorption coefficient ( $\beta$ ) and saturation intensity ( $I_s$ ) of all the samples from the following propagation equation:<sup>24</sup>

$$\frac{dI}{dz} = -\alpha(I)I, \quad (3)$$

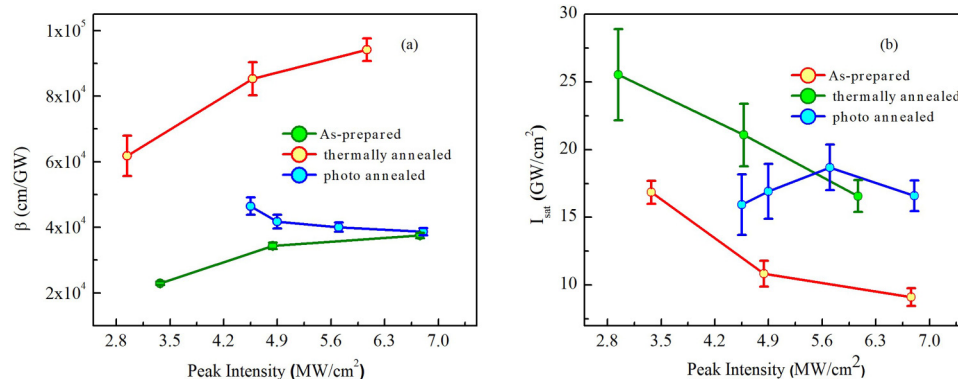


FIG. 4. (a) Variation of RSA coefficient  $\beta$  and (b)  $I_{\text{sat}}$  of three samples as a function of laser peak intensity.

where  $\alpha(I)$  is intensity dependent absorption coefficient and  $z$  is the propagation distance in the sample. Here,  $\alpha(I)$  can be written as

$$\alpha(I) = \frac{\alpha_0}{1 + \frac{I}{I_s}} + \beta_{RSA} I, \quad (4)$$

where  $\alpha_0$  is the linear absorption coefficient,  $\beta$  is the RSA coefficient, and  $I_s$  is the saturation intensity. However, normalized transmittance as a function of position  $z$  for RSA can be expressed as

$$T_N = \frac{1}{q_0 \sqrt{\pi}} \int_{-\infty}^{+\infty} \ln(1 + q_0 e^{-t^2}) dt. \quad (5)$$

Here,  $q_0 = \frac{\beta I_0 L_{eff}}{1 + \frac{I_0}{Z_0^2}}$  and  $L_{eff} = \frac{(1 - e^{-\alpha L})}{\alpha}$ , where  $I_0$ ,  $Z_0$ ,  $L$ , and  $\alpha$  are the peak intensity at the focus ( $Z=0$ ), the Rayleigh length, sample thickness, and linear absorption coefficient, respectively.<sup>23,25</sup>

RSA coefficients were extracted from the best fit of the normalized transmittance curve. The strength of RSA is determined by nonlinear absorption coefficient ( $\beta$ ). To obtain an overall picture, we plotted the variation of  $\beta$  and  $I_{sat}$  as a function of laser intensity for three different samples in Figs. 4(a) and 4(b), respectively, and the results are summarized in Table I. It can be seen that for both as-prepared and thermally annealed samples,  $\beta$  increases with laser intensity, which is a true signature of the RSA process. On the contrary, for photoannealed sample,  $\beta$  does not exhibit any significant changes against the intensity variation.  $I_{sat}$  exhibits complementary behavior to  $\beta$ , i.e., decreases with laser intensity for as-prepared and thermally annealed samples and likewise remains invariant for the optically annealed sample.

To quantify the effect of thermal and photoannealing on the non-linear optical properties, we compared the non-linear absorption coefficients  $\beta$  and  $I_{sat}$  of all the samples at comparable peak intensity. From the table, we learnt that  $\beta$  increases from  $(34\,320 \pm 980)$  cm/GW to  $(85\,310 \pm 5100)$  cm/GW after thermal annealing; whereas for photoannealed films,  $\beta$  increases to  $(46\,470 \pm 2650)$  cm/GW (Table II). Precisely, we found that  $\beta$  is significantly increased in thermally and optically annealed films

**TABLE I.** Variation of  $\beta$  and  $I_{sat}$  values with different peak intensities for as-prepared, annealed and illuminated  $\text{Ge}_{30}\text{Se}_{55}\text{Bi}_{15}$  thin films.

Sample	Intensity (MW/cm <sup>2</sup> )	$\beta$ (cm/GW)	$I_{sat}$ (GW/cm <sup>2</sup> )
As-prepared	3.4 ± 0.2	22 960 ± 530	16.8 ± 0.8
	4.8 ± 0.1	34 320 ± 980	10.8 ± 0.9
	6.8 ± 0.3	37 510 ± 810	9.1 ± 0.6
Annealed	2.9 ± 0.1	61 790 ± 6110	25.5 ± 3.3
	4.6 ± 0.2	85 310 ± 5100	21.0 ± 2.3
	6.1 ± 0.1	94 200 ± 3430	16.5 ± 1.1
Illuminated	4.5 ± 0.1	46 470 ± 2650	15.9 ± 2.2
	4.9 ± 0.2	41 750 ± 2090	16.9 ± 2.0
	5.7 ± 0.1	40 080 ± 1450	18.6 ± 1.6
	6.8 ± 0.3	38 700 ± 1080	16.6 ± 1.1

**TABLE II.** Experimentally calculated values of  $E_g$ ,  $\beta$ , and  $I_s$ .

Samples	$E_g$ (eV)	$\beta$ (cm/GW)	$I_{sat}$ (GW/cm <sup>2</sup> )
As-prepared	1.22	34 320 ± 980	10.8 ± 0.9
Annealed	0.77	85 310 ± 5100	21.0 ± 2.3
Illuminated	1.17	46 470 ± 2650	15.9 ± 2.2

compared to the as-prepared one; however, the enhancement is stronger by two times for thermally annealed samples compared to photoannealing.

Thus, the result clearly indicates that the enhancement of  $\beta$  could possibly be a direct consequence of bandgap reduction. In the literature,<sup>25,26</sup> it is shown that non-linear response (RSA) in the semiconductor follows an inverse cubic relation with bandgap, i.e.,

$$\beta^{(2)} = K^{(2)} \frac{\sqrt{E_p}}{n^2 E_g^3} \times \frac{\left(\frac{2\hbar\theta}{E_g} - 1\right)^{\frac{3}{2}}}{\left(\frac{2\hbar\theta}{E_g}\right)^5}, \quad (6)$$

where  $K^{(2)} = 3.10 \text{ eV}^{5/2} \text{ cm/MW}$  and  $E_p$  (Kane energy) are material independent constants,  $n$  is the refractive index of the material, and

the ratio  $\left[ \frac{\left(\frac{2\hbar\theta}{E_g} - 1\right)^{\frac{3}{2}}}{\left(\frac{2\hbar\theta}{E_g}\right)^5} \right]$  depends on the photon energy and bandgap,

which will help us to understand the band structure of the compound. We found from Fig. 2(b) that the bandgap decreases for thermally and optically annealed samples compared to the as-prepared sample, which leads to the enhancement of  $\beta$  as predicted from the theoretical perspective.

#### IV. CONCLUSIONS

In conclusion, we demonstrated the non-linear optical properties of  $\text{Ge}_{30}\text{Se}_{55}\text{Bi}_{15}$  thin films by open aperture Z-scan measurements. We investigated the role of thermal and photoannealing on the non-linear optical response of the sample. All the samples exhibit RSA as a function of laser intensity. Our results indicate that RSA coefficient ( $\beta$ ) increases after thermal and photoannealing, with a stronger effect observed for thermal annealing. By comparing the linear and non-linear optical properties, we conclude that the significant increase in  $\beta$  is correlated with the reduction in the optical bandgap. The observed non-linear optical absorbance is described on the basis of density of defect states and disorders present in the mobility gap. We believe that the remarkable enhancement of RSA holds tremendous potential applications in many optical devices like optical switching and limiting.

#### ACKNOWLEDGMENTS

The authors thank the Board of Research in Nuclear Science (BRNS) for financial support (Grant No. 37(3)/14/02/2016-BRNS/37016) and the Department of Physics, Indian Institute of Science Education and Research, Bhopal (IISER) for non-linear optical property study.

## REFERENCES

- <sup>1</sup>T. Wang, X. Gai, W. Wei, R. Wang, Z. Yang, X. Shen, S. Madden, and B. L. Davies, *Opt. Mater. Express* **4**, 1011 (2014).
- <sup>2</sup>J. M. Harbold, F. O. Ilday, F. W. Wise, J. S. Sanghera, V. Q. Nguyen, L. B. Shaw, and I. D. Aggarwal, *Opt. Lett.* **27**, 119 (2002).
- <sup>3</sup>D. Mandal, R. K. Yadav, A. Mondal, S. K. Bera, J. R. Aswin, P. Nemeč, T. Halenkovic, and K. V. Adarsh, *Opt. Lett.* **43**, 4787 (2018).
- <sup>4</sup>E. Stryland, H. Vanherzeele, M. Woodall, M. Soileau, A. Smirl, S. Guha, and T. Boggess, *Opt. Eng.* **24**, 613 (1985).
- <sup>5</sup>K. W. DeLong, K. B. Rochford, and G. I. Stegeman, *Appl. Phys. Lett.* **55**, 1823 (1989).
- <sup>6</sup>C. R. Mendonca, D. S. Correa, F. Marlow, T. Voss, P. Tayalia, and E. Mazur, *Appl. Phys. Lett.* **95**, 113309 (2009).
- <sup>7</sup>S. Binu, P. Khan, A. R. Barik, R. Sharma, R. Golovchak, H. Jain, and K. V. Adarsh, *Mater. Res. Express* **1**, 045025 (2014).
- <sup>8</sup>A. Prasad, C. Zha, R. P. Wang, A. Smith, S. Madden, and B. L. Davies, *Opt. Exp.* **16**, 2804 (2008).
- <sup>9</sup>K. Ogusu, J. Yamasaki, S. Maeda, M. Kitao, and M. Minakata, *Opt. Lett.* **29**(3), 265 (2004).
- <sup>10</sup>S. Dai, F. Chen, Y. Xu, Z. Xu, X. Shen, T. Xu, R. Wang, and W. Ji, *Opt. Exp.* **23**, 1300 (2015).
- <sup>11</sup>Y. Huang, F. Chen, B. Qiao, S. Dai, Q. Nie, and X. Zhang, *Opt. Mater. Express* **6**, 1644 (2016).
- <sup>12</sup>F. Smektala, C. Quemard, V. Couderc, and A. Barthelemy, *J. Non-Cryst. Solids* **274**, 232 (2000).
- <sup>13</sup>M. Behera, R. Naik, C. Sripan, R. Ganesan, and N. C. Mishra, *Curr. Appl. Phys.* **19**, 884 (2019).
- <sup>14</sup>P. K. Jain, Deepika, and N. S. Saxena, *Philos. Mag.* **89**, 641 (2009).
- <sup>15</sup>A. Aparimita, M. Behera, C. Sripan, R. Ganesan, S. Jena, and R. Naik, *J. Alloys Comp.* **739**, 997 (2018).
- <sup>16</sup>R. Panda, M. Panda, H. Rath, U. P. Singh, R. Naik, and N. C. Mishra, *Opt. Mater.* **84**, 618 (2018).
- <sup>17</sup>J. Tauc, *Amorphous and Liquid Semiconductors* (Plenum Press, New York, 1979).
- <sup>18</sup>N. F. Mott and E. A. Davis, *Electronic Processes in Non-Crystalline Materials* (Clarendon Press, Oxford, 1971).
- <sup>19</sup>P. Khan, A. R. Barik, E. M. Vinod, K. S. Sangunni, H. Jain, and K. V. Adarsh, *Opt. Exp.* **20**(11), 12416 (2012).
- <sup>20</sup>P. Khan, R. Sharma, U. Deshpande, and K. V. Adarsh, *Opt. Lett.* **40**, 1559 (2015).
- <sup>21</sup>P. Khan, H. Jain, and K. V. Adarsh, *Sci. Rep.* **4**, 4029 (2015).
- <sup>22</sup>H. I. Elim, J. Yang, and J. Y. Lee, *Appl. Phys. Lett.* **88**, 083107 (2006).
- <sup>23</sup>P. Pradhan, P. Khan, J. R. Aswin, K. V. Adarsh, R. Naik, N. Das, and A. K. Panda, *J. Appl. Phys.* **125**, 015105 (2019).
- <sup>24</sup>M. S. Bahae, A. Said, T. H. Wei, D. J. Hagan, and E. V. Stryland, *IEEE J. Quantum Electron.* **26**, 760 (1990).
- <sup>25</sup>A. Rana, J. Aneesh, Y. Kumar, M. S. Arjunan, K. V. Adarsh, S. Sen, and M. P. Shirage, *Appl. Phys. Lett.* **107**, 231907 (2015).
- <sup>26</sup>E. Stryland, M. Woodall, H. Vanherzeele, and M. J. Soileau, *Opt. Lett.* **10**, 490 (1985).